Contents lists available at [ScienceDirect](https://www.sciencedirect.com)

Waste Management

journal homepage: www.elsevier.com/locate/wasman

Shear strength characterization of fresh MBT and MSWI wastes from a Spanish treatment facility

Pablo Lapeña-Mañero ^{a, b, *}, Carmen García-Casuso ^{a, b}, Jorge Cañizal ^c, César Sagaseta ^c^a Department of Civil Engineering, Universidad Católica de la Santísima Concepción, Alonso de Rivera 2850, 4090541, Concepción, Chile^b Formerly Department of Ground Engineering and Material Science, Universidad de Cantabria, Avda. de los Castros s/n, 39005 Santander, España^c Department of Ground Engineering and Material Science, Universidad de Cantabria. Avda. de los Castros s/n, 39005 Santander, España

ARTICLE INFO

Keywords:

Mechanical and Biological Treatment
Municipal Solid Waste Incineration
Shear strength characterization
Laboratory testing
Municipal Solid Waste

ABSTRACT

A laboratory shear strength characterization of the landfilled materials of the Municipal Solid Waste integral treatment plant from the Meruelo Environmental Complex in Cantabria (Spain) was performed. The materials tested come from the rejection of the Mechanical and Biological Treatment (MBT-MSW) and the slags produced in the energy recovery plant (MSWI). Laboratory characterization consisted of direct shear and consolidated drained triaxial testing. Mohr-Coulomb failure criterion parameter values were obtained and compared to reported values in the literature. In some tests, failure was not reached due to the reinforcement effect for fibrous particles; thus, the mobilized shear strength parameters for different values of axial strain were obtained. The triaxial test results showed strain-hardening in MSW-MBT but not in MSWI. Failure was reached on both materials in direct shear testing, with MSWI showing peak and ultimate strengths, whereas MBT-MSW exhibited only ultimate strength. Direct shear test obtained strength can be characterized by a cohesion of 20 kPa and a friction angle of 33° for MBT-MSW ultimate strength, while cohesion and friction angle varies from 13.4 to 29 kPa and from 38.5° to 42.3° for MSWI ultimate and peak strength, respectively. The mobilized cohesion and friction angle obtained for MBT-MSW in consolidated drained triaxial tests ranged from 15.1 to 62.7 kPa and 20° to 28.7°, corresponding to a strain level of 5% and 25%, respectively. In triaxial testing of MSWI specimens, failure was reached, and the material showed a cohesion of 51.3 kPa and a friction angle of 32.8°.

Abbreviations

MBT-MSW	Mechanically and Biologically Treated Municipal Solid Wastes
MSW	Municipal Solid Waste
MSWI	Municipal Solid Waste Incineration
MBT	Mechanical and Biological Treatment
SOW	Stabilized Organic Waste
SRF	Solid Recovered Fuel
ϕ	Friction angle
c	Cohesion
ψ	Dilatancy angle
γ	Unit weight
σ'	Effective normal stress
τ	Shear stress
d_x	Shear displacement in direct shear tests
d_v	Vertical displacement in direct shear tests

p'_0	Effective cell pressure in triaxial tests
ε_a	Axial strain
ε_v	Volumetric strain
ε_a^p	Plastic axial strain
ε_v^p	Plastic volumetric strain

1. Introduction

The management of the increasing quantity of produced waste is a problem in modern societies. Despite the efforts in reducing and recycling the generated residues, a significant fraction ends up in sanitary landfills (Velis et al., 2010). Moreover, the current environmental awareness of the population makes it challenging to establish new landfill facilities. Due to that, some sanitary landfills currently in operation are receiving more waste than expected, and consequently, they are growing in height and increasing their slope angles. Notwithstanding

MBT-MSW, Mechanically and Biologically Treated Municipal Solid Wastes

* Corresponding author.

E-mail address: plapenamanero@gmail.com (P. Lapeña-Mañero).<https://doi.org/10.1016/j.wasman.2022.08.026>

Received 4 February 2022; Received in revised form 5 July 2022; Accepted 27 August 2022

0956-053/© 20XX

the efforts to make these new geometries safe, landfill slope instabilities continue to occur. There are several well-documented accidents around the world, like those that occurred in the Kettleman Hills landfill in California (Mitchell et al., 1993), Rumpke landfill in Ohio (Eid et al., 2000; Stark et al., 2000; Chugh et al., 2007), Doña Juana Landfill in Colombia (Caicedo et al., 2002), Payatas landfill in the Philippines (Merry et al., 2005; Huvaj-Sarihan and Stark, 2008), Gnojna Grora landfill in Poland (Huvaj-Sarihan and Stark, 2008), Hiriya landfill in Israel (Huvaj-Sarihan and Stark, 2008), Leuwigajah landfill in Indonesia (Lavigne et al., 2014), Shenzhen landfill in China (Peng et al., 2016) and Santa Marta landfill in Chile (Espinace and Farfán, 2016), among others. An appropriate geotechnical design of the slopes is fundamental to prevent these accidents from occurring, and thus the knowledge of the mechanical properties of the material that makes up a sanitary landfill is required.

Furthermore, European Council Directive 1999/31/EC on the landfill of waste (European Council, 2018) establishes the conditions for residue disposal in landfills in the European Union and the necessity to reduce the amount of biodegradable matter in the waste mass. The directive also makes it compulsory to subject the waste to be landfilled to treatment prior to its disposal. Although the directive mainly focuses on reducing the polluting potential, it also states the necessity of ensuring the “stability of the mass of waste and associated structures, particularly in respect of avoidance of slippages”.

Mechanical and biological treatments (MBT) consist of a combination of processes applied to the residue in order to reduce the adverse consequences of landfill disposal. These techniques are designed to meet the criteria established in the 1999/31/EC directive, and thus their main objectives are to stabilize and reduce the amount of organic matter in the waste mass, to reduce the volume and mass of the disposed waste, and to reduce the production of pollutants. As a result, most of the studies found in the literature on the properties of Mechanically and Biologically Treated Municipal Solid Wastes (MBT-MSW) are focused on the physicochemical properties of the treated residue rather than on its mechanical behavior. These studies show significant variability in terms of physical and chemical characteristics depending both on the composition of the untreated waste and on the type of mechanical and biological treatments applied (Rotter et al., 2004; Fricke et al., 2005; Robinson et al., 2005; Pimolthai, 2010; Velis et al., 2010; Di Lonardo et al., 2012; López et al., 2018; Molleda et al., 2020). Due to that variability, a site-specific characterization of the MBT-MSW is recommended (Di Lonardo et al., 2012).

As MBTs are designed to improve the quality of the waste from a physicochemical point of view, it is not yet clear how these treatments affect the mechanical properties of Municipal Solid Waste (MSW). The great variety of treatments covered under the MBT designation makes it harder to determine this influence as a general trend, and hence the effect of each kind of treatment must be studied independently.

In this work, MBT-MSW and MSWI wastes from a mechanical and biological treatment facility in northern Spain are studied to obtain their mechanical properties using traditional geotechnical tests such as large direct shear and triaxial tests.

2. Waste mechanical behavior

Although there are clear differences between MSW and soils in terms of origin, composition and mechanical behavior, the stability of landfills is traditionally studied using methods and models devised for soils. One of the most relevant differences in the behavior of both materials is that MSW particles cannot be considered infinitely rigid in comparison with the waste mass, and thus the deformation of the material is not caused only by the change in pore volume as it occurs in regular soils (Grisolia and Napoleoni, 1996; Dixon and Jones, 2005; Karimpour-Fard et al., 2011). Besides, waste behavior changes with their degradation, and hence with time. Although initial studies carried

out by Landva and Clark (1990) indicated that aging does not influence the value of shear strength parameters, currently, most authors suggest that aging produces the material to become more frictional, with increasing Mohr-Coulomb’s model friction angle and decreasing cohesion with time (Grisolia and Napoleoni, 1996; Eid et al., 2000; Dixon and Jones, 2005; Zhan et al., 2008; Karimpour-Fard et al., 2011; Gomes et al., 2013; Abreu and Vilar, 2017; Feng et al., 2017; Pulat and Yukselen-Aksoy, 2017; Ramaiah et al., 2017). Nevertheless, there is no consensus about this trend, with some authors stating that only the friction angle increases with aging and cohesion remains constant (Bareither et al., 2012) and others that both parameters increase with time (Zhao et al., 2014).

It is well established that raw MSW show large deformability and that the deformation required to reach yielding is often much higher than the allowable deformation of other components of the landfill (Sánchez-Alciturri et al., 1993; Grisolia and Napoleoni, 1996; Stark et al., 2000). Accordingly, most authors recommend the usage of mobilized shear strength parameter values instead of the maximum values obtained traditionally in the tests (Eid et al., 2000; Stark et al., 2000; Zhan et al., 2008; Bray et al., 2009; Reddy et al., 2009). Furthermore, due to the great deformability of the material, failure is often not reached during conventional laboratory and in-situ geotechnical tests (Grisolia and Napoleoni, 1996; Dixon et al., 2006; Abreu and Vilar, 2017). Most authors also indicate that the material shows strain-hardening, with an upward concave curvature of the stress-strain curves in direct shear and triaxial tests (Sánchez-Alciturri et al., 1993; Dixon et al., 2006; Zhan et al., 2008; Stark et al., 2009; Karimpour-Fard et al., 2011; Bareither et al., 2012; Gomes et al., 2013; Abreu and Vilar, 2017; Feng et al., 2017; Ramaiah et al., 2017).

MSW behave as frictional materials, with increasing strength with the mean normal octahedral stress, and hence the Mohr-Coulomb failure criterion is often used (Landva and Clark, 1990; Dixon and Jones, 2005; Bray et al., 2009; Bareither et al., 2020). Nevertheless, the strength increase with depth is not linear. The relationship between strength and depth can be represented with a curve with a declining slope, indicating that the friction angle value decreases with depth. This behavior is similar to that shown by granular soils. Some authors propose the usage of bi-linear (Kavazanjian et al., 1995), tri-linear (Manassero et al., 1996), or curved Mohr-Coulomb envelopes (Dixon and Jones, 2005; Zekkos et al., 2007b; Stark et al., 2009).

The material is usually studied like a drained material, at least in static scenarios, and its behavior is similar to that observed in granular soils, with low or even negligible cohesion (Palma, 1995; Stark et al., 2009; Pulat and Yukselen-Aksoy, 2017). Notwithstanding the sand-like behavior, the apparent cohesion obtained in the experimental characterization of MSW can be explained by the reinforcement effect of the fibrous materials present on the waste mass (Eid et al., 2000; Feng et al., 2017; Machado et al., 2002; Kölsch, 1995). Unlike the cohesive behavior shown by other materials, the reinforcement effect of fibers only appears with high strains, with the development of tensile forces in the fibers that contribute to the shear strength of the material (Zhan et al., 2008; Gomes et al., 2013; Bareither et al., 2020). Because of this reinforcement effect, the strength of MSW is influenced by the relative quantity of fibrous particles in the waste mass. As a general trend, the material shear strength increases with fiber content, but it reaches a maximum when the slippage between fibers makes shear strength decrease (Grisolia and Napoleoni, 1996). The ranges of friction angle (ϕ) and cohesion (c) reported in the literature are wide, with ϕ ranging from 19° to 53° and c between 0 and 70 kPa.

Unit weight of MSW increases rapidly and significantly with depth as a consequence of the auto compaction produced by its weight and the decomposition of organic matter. The reported values in the literature range from 8 to 12 kN/m³ for near-surface materials and from 15 to 18 kN/m³ in deeper areas. The unit weight of the residues on landfills subjected to leachate recirculation (bioreactors) is higher, with re-

ported values from 9 to 16 kN/m³ for shallow areas and 18 to 22 kN/m³ for greater depths (Kavazanjian et al., 2001). Zekkos et al. (2006) proposed a hyperbolic model for the unit weight in a landfill that depends on the near-surface in-place unit weight, the depth, and the particular operation procedures of the landfill.

Despite the variability of the reported geotechnical properties for MSW and the high degree of heterogeneity of the waste mass that makes up a landfill, the geotechnical properties vary consistently and predictably, which makes geotechnical modeling of landfill plausible (Sánchez-Alciturri et al., 1993; Palma, 1995; Dixon and Jones, 2005).

In spite of the significant research on MSW mechanical properties developed in the last decades, there is a scarcity of information on the behavior of the residues when subjected to mechanical and biological pre-treatments. Furthermore, some studies do not report the type of treatment or even whether the material has been treated before landfilling or not. This absence of information makes it challenging to identify the changes that the treatments produce on the material.

Most authors agree that MBT reduces the heterogeneity of residues and their deformability due to the reduction in grain size and the sorting process usually associated with the treatment (Bhandari and Powrie, 2013). Since the amount of organic matter is reduced during the process, the long-term settlement caused by its degradation is also reduced (Siddiqui et al., 2013). On the contrary of what was reported for raw MSW, some studies indicate that it is possible to reach failure within the strain range that is typically achieved in geotechnical tests (Bhandari and Powrie, 2013), while others indicate the contrary (Sivakumar Babu et al., 2015; Lakshmikanthan et al., 2018). The treatment also increases the unit weight of the material (Siddiqui et al., 2013), just like it was reported for bioreactor landfills. The initial unit weight of the samples influences the shear strength obtained from laboratory tests, both when failure is not reached (Sivakumar Babu et al., 2015) and when peak or ultimate strength is reached (Bhandari and Powrie, 2013). Despite the reduction in the amount and length of fibers, the amount of fibrous material in the waste mass is still relevant. The existence of this kind of particle gives rise to an apparent cohesion like it was observed in raw MSW (Fucale et al., 2015).

Another common treatment applied to MSW is incineration (MSWI). The residues produced in this process are also disposed in landfills, and thus their geotechnical properties should be investigated. Incineration can be applied directly to regular MSW or to the material that has undergone previous treatment. Le et al. (2017) characterized the bottom ash produced by a Municipal Solid Waste Incineration (MSWI) facility and concluded that the behavior in terms of strength and deformability is similar to that of dense sands. Zekkos et al. (2013) studied the MSWI ash from a Michigan monofill and found that the shear strength and the in-situ shear wave velocities were higher than those expected from sandy or gravely soils and attributed this behavior to the ash cementation seen on the site. The authors also report that the response of the material to triaxial testing was different depending on the degree of saturation of the specimens during the tests.

3. Materials studied

This study tested two different fresh materials obtained directly from the stockpiles at the MSW integral treatment plant from the Meruelo Environmental Complex in Cantabria (Spain): the rejected fraction of the refinement stage (MBT rejection) and the slags produced in the energy recovery plant (MSWI slag). Both materials, along with the mechanical and biological treatment applied to the residue, are described below.

3.1. Treatment description

In the area of influence of the treatment facility, cardboard, paper, glass, and light packaging are collected separately, but not the organic

fraction, which is incorporated into the rest fraction. Only this latter waste stream is treated on the plant.

The first step of the MBT consists of the manual separation of the glass and the voluminous materials contained in the rest fraction; the mainstream is then screened using a 100-mm trommel. Next, the over-size fraction is subjected to manual and automatic extraction of recyclable materials, and the rest is used as Solid Recovered Fuel (SRF) in the energy recovery plant. The material that passes through the trommel contains most organic matter, and it is sent to the biological treatment facility to obtain Stabilized Organic Waste (SOW). The biological treatment is carried out in two covered units and consists of an eight-week-long aerobic composting process with weekly mixing using an automatic turning machine and with no water addition. Next, the resulting material is sent to the refinement plant, shredded, and screened using a 9-mm trommel. Three different streams are generated in the refinement plant: compost, high calorific fraction, and low calorific fraction. Only the latter is considered a rejection of the refinement stage, as the compost and the high calorific fraction are used as SRF in the energy recovery plant. Finally, the rejected fraction from the refinement plant and the slags produced in the energy recovery plant are sent to the landfill.

3.2. MBT rejection

MBT rejection is one of the landfilled materials, and thus it was studied in this investigation. A picture of the material on its arrival to the laboratory is shown in Fig. 1a.

A complete physicochemical characterization of the MBT rejection can be found in Molleda (2017). According to the author, moisture content and volatile solids are season-dependent. On a sampling performed in February, they obtained a 30% moisture content and a 57% of volatile solids. Regarding the particle size distribution of the material, only three fractions were identified, with 15% in mass with grain size larger than 20 mm, 78% between 4 and 20 mm, and 7% smaller than 4 mm. Most materials with particles larger than 20 mm are glass and ceramics (58%) and plastics and cardboard (24%). A summary of the composition and the particle size distribution obtained by Molleda (2017) is included in the Supplementary Material (Table A.1).

3.3. MSWI slag

The residues produced in the energy recovery plant (Fig. 1b) are landfilled along with the rejection from the refinement plant. This material was also studied by Molleda (2017) from a physicochemical point of view (see Table A.1 in the Supplementary Material). The material's reported moisture and volatile solids content are significantly lower than in the case of the rejection, with 15% and 5%, respectively. As for the particle size distribution, 22% of the mass corresponds with particles larger than 20 mm, 44% with particle sizes between 4 and 20 mm, and 34% with particles smaller than 4 mm.

4. Testing methodology

The standard equipment and procedures of geotechnical tests were adapted for testing MSW. The testing methodology and the modifications performed to the equipment are described below.

4.1. Sampling

Separate samples for each material were collected and sieved on-site to remove particles larger than 20 mm, as this is the maximum allowable grain size of the testing equipment used in this project. Scalping, shredding, or a combination of both are commonly used techniques to reduce maximum particle size in waste mechanical testing (Bareither et al., 2012). The removal of larger particles does not significantly affect

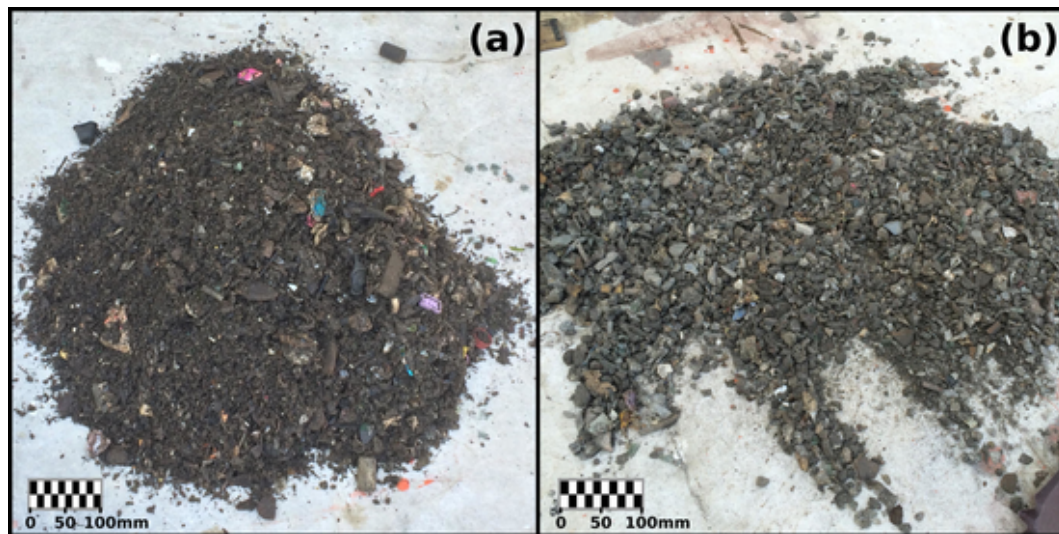


Fig. 1. Pictures of the studied materials, a) MBT rejection, and b) Slag from the energy recovery plant.

the results obtained in the shear strength characterization of sand-like materials for percentages of scalped material lower than 20–30% (Bareither et al., 2008; Dorador and Villalobos, 2020). The material rejected after sieving was less than 10% of the total amount of the initially collected sample, and thus the sample can be considered representative for both materials. Upon arrival to the laboratory, samples for each material were mixed, homogenized, and stored in high-resistance plastic bags.

4.2. Specimen initial unit weight selection and compaction procedure

Some authors suggest that the initial unit weight of the specimens influences geotechnical testing results (Bhandari and Powrie, 2013; Sivakumar Babu et al., 2015), and hence it is important to prepare specimens with similar conditions to those found in situ. Although the waste is compacted at its disposal using a landfill compactor, the resulting unit weight is not measured. Therefore, compaction tests were performed on both materials to establish and standardize the initial unit weight for specimen preparation. Five MBT rejection specimens were compacted with the same energy used in the standard effort Proctor test with their natural water content. The initial unit weight was established assuming that the in-situ unit weight is 95% of the average value obtained in the compaction tests. With these conditions, all MBT rejection specimens tested in this investigation were prepared with an initial unit weight of 12.5 kN/m³.

The Proctor compaction method produced MSWI slag particles to break, significantly affecting the obtained results. Due to that, the static compression response of both materials was compared, and the initial unit weight of incineration slags was established to that obtained under the same load that produced the specimen unit weight for the MBT rejection. With this criterion, the initial unit weight used for MSWI slag specimen preparation was 15.4 kN/m³.

4.3. Large direct shear tests

Tests were performed per the Spanish standard UNE-103401:1998, with modifications to the testing procedures and equipment. The procedures described in the Spanish standard are in accordance with that outlined in ASTM D6528-17. A 300x300 mm shear box with a maximum vertical and horizontal load capacity of 100 kN was used to conduct the direct shear testing campaign. The equipment used in this investigation provides the vertical load with a hydraulic system, and it was difficult to accurately apply loads, especially for low vertical pressure. An additional load cell was added between the shear box and the

vertical loading frame to improve accuracy in the application of the vertical load. A cross-section of the shear box, indicating all relevant dimensions, can be found in Figure A.2 (Supplementary Material). Besides, due to the large displacement before yielding expected, the horizontal axis was modified to increase the maximum allowable movement to over 100 mm. This improvement entailed the elimination of the watertight container around the shear box, which made it not possible to test the material saturated. However, as both materials behave like frictional soils, they can be tested in non-saturated conditions without the risk of developing suction in the pores.

Furthermore, due to the great compressibility of the material, an extension was attached on top of the shear box to accommodate the sample before compaction in the specimen preparation process. The addition of the vertical load cell and the shear box extension required installing longer rods on the vertical load application frame. A full description of the device improvements can be found in Lapeña-Mañero (2017).

As described before, MSWI particles tend to break when compacted using dynamic compaction methods. Due to that, all specimens were compacted directly in the shear box using static compression to avoid particle breakage on this material and standardize the compaction method between specimens. Compaction load was applied with the same equipment used to provide the vertical load during the tests. For MSWI slag samples, the material had to be previously compacted by rodding, as it was hard to reach the target unit weight only by applying static pressure. Athanasopoulos (2008) established some guidelines for MSW laboratory testing based on a literature review. The author advises against the usage of rodding for MSW compaction, given that it could break the fibers present in the waste, changing their behavior. However, the tested slags do not contain fibers, so there is no risk of this phenomenon occurring. Although, in the same work, Athanasopoulos (2008) also reports static compaction not reproducing the on-landfill conditions appropriately in some scenarios, the usage of this technique in the present investigation was successful, attaining the target unit weight on every test. With the conditions described above, specimens were prepared in three equal layers, monitoring compaction load during the whole process using the vertical load cell. Spacers with the appropriate length along with a loading cap larger than the shear box internal cross-section were used to control the height of each layer by creating a physical end-stop for compaction. Full contact between the modified loading cap and the top of the extension was verified visually and using the vertical load cell readings. Once full contact was reached, the load was maintained constant for 20 min before fully removing the vertical load, the modified loading cap, and the spacer to extend and

compact the next layer. After compaction, the original loading cap was installed to initiate the consolidation stage. The observed behavior of residues during consolidation differs from that observed in conventional soils, without stabilizing specimen height even for long periods. Besides, in direct shear apparatus, it is not possible to measure pore pressure, and thus it is not possible to establish the end of primary consolidation in this manner. Due to that, the duration of the consolidation stage in direct shear testing was established based on the information obtained in the consolidation stage of the triaxial test performed on the materials. In these tests, it was observed that the total dissipation of the excess pore water pressure depends on the applied confining pressure, with longer consolidation times for specimens subjected to higher confining pressures. Based on the information gathered in triaxial testing, consolidation time was established in 24 h for tests with normal stress lower or equal to 50 kPa and 48 h for the rest of the tests.

The MBT rejection expelled leachate during consolidation and percolated outside the shear box. As the watertight container was removed from the equipment to increase the maximum possible horizontal displacement, a stainless-steel element was added to the contour of the direct shear apparatus to prevent the leachate from getting in contact with the electronic and hydraulic systems. The sealant had to be replaced regularly as the leachate disintegrated it.

Finally, shear displacement at a constant rate was applied to the specimen. Shear displacement rate is usually obtained from the analysis of the consolidation stage. However, as residues behave differently than regular soils during consolidation, it is not possible to apply the habitual procedures to obtain the shear displacement rate. Therefore, the shear displacement rate was established at 1 mm/min, a value commonly found in the literature for MSW direct shear testing.

4.4. Triaxial compression tests

Tests were performed in accordance with the Spanish standard UNE-103402:1998 in consolidated-drained conditions over specimens 100 mm in diameter and 200 mm long. The standard corresponds with ASTM D7181-20, and most of the procedures described in both standards are analogous. On the first tests carried out in the present investigation, the specimens' upper face did not stay horizontal after the consolidation stage, which aggravated in the posterior deviator stress application phase (Lapeña-Mañero, 2017). To address this issue, the ending part of the loading ram and the top cap were redesigned to limit the inclination of the upper face of the specimen (see Figure A.3 in the [Supplementary Material](#)). Due to the difficulties in manufacturing the top cap drainage channels, only bottom drainage was allowed on the tests. Bottom drainage channels were connected to a high-volume automatic volume change device to monitor the volume change in consolidation and deviator stress application stages.

Specimens were prepared in two-part compaction molds with a procedure analogous to the one described for direct shear testing, with a larger loading cap and spacers to limit the height of each layer. Due to the slenderness of the specimens, the material was compacted using five equal layers instead of three. Once the specimen was compacted, it was necessary to remove it from the mold and encase it with a rubber membrane. To avoid damaging the specimens in the membrane installation process, it was decided to freeze specimens before releasing them from the molds. As saturating the specimens properly in the compaction molds was not possible for both materials, specimens were prepared directly saturated. After compaction, to prevent specimen expansion on freezing, a grid was installed on top of the upper face of the specimen, held in place by the mold extension. Specimens were frozen at -18°C for at least 24 h before being demolded and placed inside the triaxial cell for testing. Pictures of the process are shown in the [Supplementary Material](#) (Figure A.4). Particle size analyses were performed on samples of both materials before and after undergoing the specimen preparation process to ensure that it produced no significant change in the material

physical properties. These specimens were prepared specifically for this purpose; thus, they were not subjected to the following test stages. In all cases, results indicate no change in the particle size distribution of the samples.

As the specimen was placed inside the triaxial cell frozen, a defrost phase was added before the standardized stages. Specimens were left for 24 h at room temperature with a cell pressure lower than the effective cell pressure used in the posterior test stages. A confining pressure between 35 and 40 kPa was used for all specimens during the defrosting phase. After defrosting, back pressure was increased in steps to 600 kPa maintaining constant the effective cell pressure to improve saturation. The behavior of the specimens in the consolidation stage differed from regular soils, without a clear stabilization of volume change even within extensive periods. Due to that, consolidation time and deviator application rate were obtained considering excess pore pressure development instead of the volume change. During consolidation, several backpressure checkings were performed by closing the drainage valve and measuring pore pressure change over time. Based on this data, consolidation time and axial deformation rate were established. Different consolidation phase durations were used depending on the test cell pressure (p'_0): 24 h for $p'_0 = 50$ kPa, 48 h for $p'_0 = 150$ kPa, and 72 h for $p'_0 = 300$ kPa. After consolidation, axial deformation was applied at a constant 0.1 mm/min rate for all cell pressures. Strain rate is reported to significantly affect the results obtained in shear strength tests on MSW (Zekkos et al., 2007a). The strain rate was determined for the worst-case scenario and applied to all specimens to avoid this effect and to obtain comparable results from the tests. To ensure that the drained conditions were met, the drainage valve was closed right after stopping the application of deviator stress and pore water pressure variation was measured, resulting negligible for all tests. Considering the great deformability before yielding showed typically by MSW, tests were continued until 30% strain was reached even though the UNE-103402:1998 standard establishes a maximum axial strain of 20%.

5. Results and discussion

5.1. Moisture content

As usual in geotechnical engineering for soils with a significant organic matter content, moisture content was obtained by oven-drying the samples at 60°C . Moisture content was obtained from the samples upon arrival to the laboratory before specimen preparation. Little variation of the measured moisture content over time was found. For the MBT rejection, the measured moisture content was in the range of 40% to 49%, with an average value of 42%. MSWI slags moisture content was in the range of 7% to 17%, with an average value of 15%.

5.2. Particle size distribution

Particle size distribution tests were performed regularly on the samples on their arrival to the laboratory, and it remained almost constant over time. It is necessary to state that the samples tested in the laboratory had been previously screened on-site to remove particles larger than 20 mm. According to the characterization performed by Molleda (2007) and summarized in Table A.1, the amount of material with particle size larger than 20 mm is 15% and 22% for the MBT rejection and the MSWI slags, respectively. Particle-size distribution curves for both materials are plotted in Fig. 2. MBT rejection particles are smaller than MSWI slag particles, and both materials contain a negligible amount of fine material.

5.3. Direct shear tests

For direct shear testing, specimens with the effective normal stress of 15, 30, 50, 150, and 300 kPa were tested for each material.

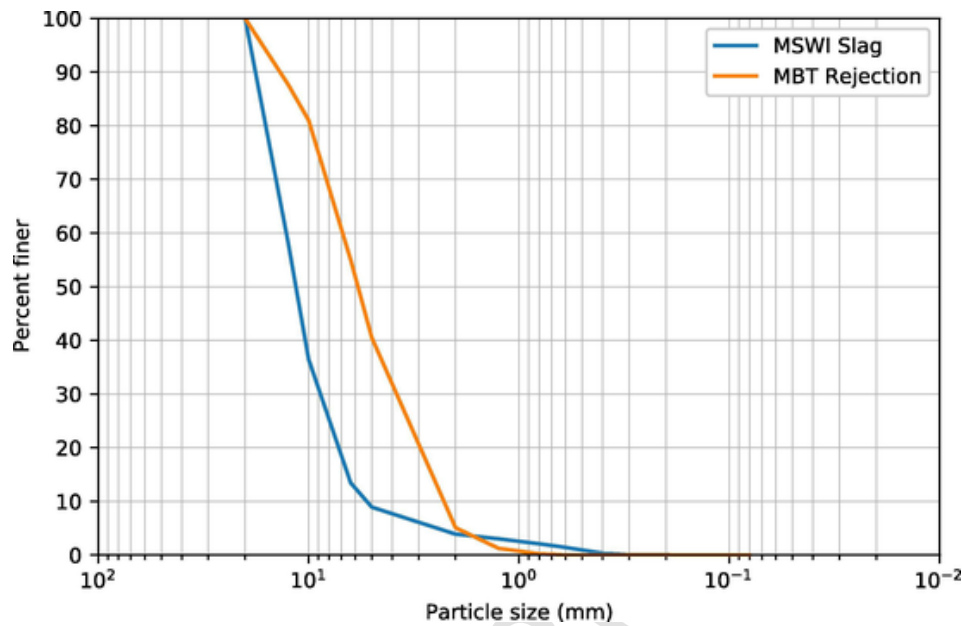


Fig. 2. Representative particle-size curves for the two materials studied.

5.3.1. MBT rejection

Shear stress and change in height against shear displacement curves for all tested MBT rejection specimens are plotted in Fig. 3a and 3b, respectively. As shown in Fig. 3a, in all tested specimens a maximum value of shear-stress (τ) was observed for the horizontal displacement induced during the tests. The points of maximum τ are pointed out in the figure with circles. In most cases, the maximum value remained constant with increasing horizontal displacement. However, the specimen with $\sigma' = 300$ kPa showed a small decrease in shear stress for a shear displacement of about 70 mm, which is likely due to problems associated with high displacements. Due to that, and according to the general behavior of the specimens and the volume change of this particular specimen during the test (see Fig. 3b), the maximum attained stress was considered the ultimate stress, like in all other specimens. Fig. 3a indicates that maximum strength is mobilized for higher strains for specimens with higher normal stress.

On the other hand, Fig. 3b indicates that specimens with effective normal stress up to 50 kPa ($\sigma' = 15$ kPa, $\sigma' = 30$ kPa, and $\sigma' = 50$ kPa) showed positive dilatancy while the rest ($\sigma' = 150$ kPa and $\sigma' = 300$) behaved as a contractive material, indicating that the specimens with effective normal stresses lower than 50 kPa were over-consolidated and the two specimens tested at higher effective normal stresses were normally consolidated. The overconsolidated behavior of some samples indicates that the static compaction procedure applied for specimen preparation produced a preconsolidation pressure larger than 50 kPa and lower than 150 kPa, which is consistent with the measurements taken during compaction. Numerical values of dilatancy angle for every tested specimen are listed in Table A.10 in the Supplementary Material.

The points of maximum stress have been plotted in Mohr's plane to obtain strength envelopes. Data adjust reasonably well to a straight line (see Figure A.6 in the Supplementary Material); thus, the Mohr-Coulomb failure criterion could be used. Nevertheless, as found in the literature review, the failure envelope of MSW can also be described using non-linear envelopes. One traditional approach is to consider the envelope an effective stress potential function (Perry, 1994), which in its simplest form can be expressed using equation (1).

$$\tau = A \cdot \sigma'^b \quad (1)$$

A and b are model fit parameters with no physical meaning. This may cause dimensional issues with the usage of this type of envelope, both in the process of value parameter determination and in later usage. Several authors have proposed variations of equation (1) to deal with these problems (Jiang et al., 2003; Yang et al., 2013). However, the proposed expressions add unnecessary complexity to the analysis without improving accuracy and thus they were not used in the present investigation.

Another approach for considering the nonlinearity of the failure envelope is to use a modified expression derived from the Mohr-Coulomb criterion. Various authors have proposed this kind of criterion for different types of materials, such as rock joints (Barton, 1976), geotextiles and geomembranes (Martínez-Bacas et al., 2011), and soils (Maksimovic, 1989). Zekkos et al. (2010) proposed a model for MSW considering that the friction angle decreases linearly with the natural logarithm of the normal stress. With this assumption, the strength envelope can be expressed with equation (2).

$$\tau = c + \sigma' \cdot \tan \left(\phi_0 - \Delta\phi \cdot \log \left(\frac{\sigma'}{P_a} \right) \right) \quad (2)$$

Where P_a is the value of atmospheric pressure (reference pressure), ϕ_0 is the friction angle at $\sigma' = 1$ atm (101.3 kPa), and $\Delta\phi$ represents the rate of reduction of the friction angle with the normal stress. Figures with the adjustments along with the values of the parameters of the three described models for the studied material are included in the Supplementary Material (see Figure A.5 and Table A.10).

5.3.2. MSWI slag

Fig. 3c shows the shear stress against the shear displacement curves for all MSWI slag tested specimens, with triangles representing peak stress and circles ultimate stress. In Fig. 3d, the change in height against the shear displacement is plotted, showing that all the specimens increased their volume during the tests. As reported by other authors for similar materials (Zekkos et al., 2013; Le et al., 2017), the residue from the incineration facility behaved as dense sand, with both peak and ultimate strength. Finally, the sets of strength points were plotted in the Mohr plane, and the models described above for the rejection were adjusted. Figures with the adjustments (Figures A.8 y A.9) and numerical values of the strength parameters and dilatancy

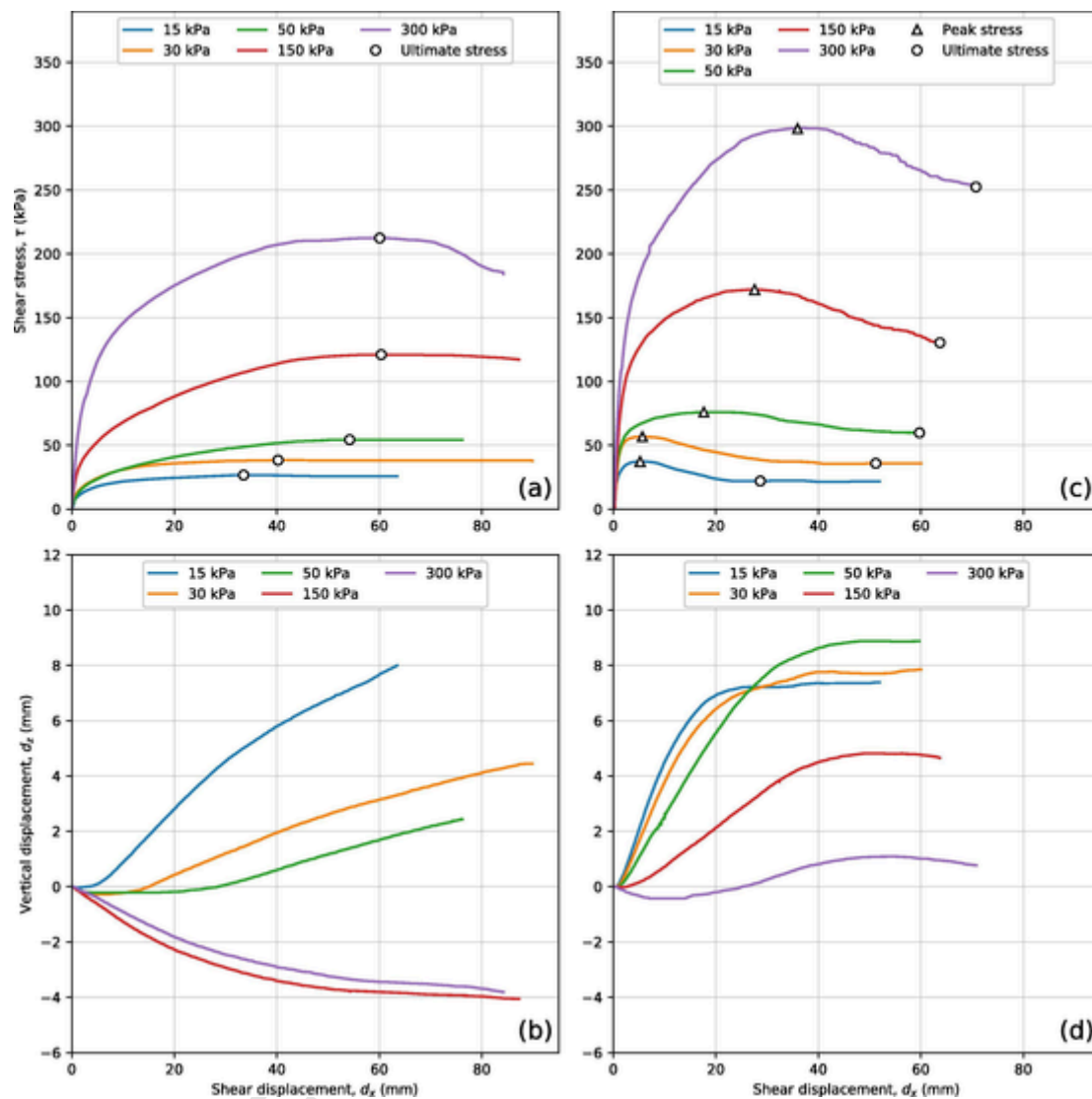


Fig. 3. Direct shear test results, a) shear stress vs. horizontal displacement curves for rejection specimens, b) vertical displacement vs. horizontal displacement curves for rejection specimens, c) shear stress vs. horizontal displacement curves for MSWI slag specimens, and d) vertical displacement vs. horizontal displacement curves for MSWI slag specimens.

angle values obtained for each specimen (Table A.10) are presented in the [Supplementary data](#).

5.3.3. Comparison with reported results

The value ranges for cohesion and friction angle for residues found in the literature are wide, with cohesion ranging from 0 to 64 kPa, whereas friction angle value range is between 15.7° and 48.1° (see Fig. 4). Direct shear test results found in the literature are summarized in Fig. 4, along with the Mohr-Coulomb parameter values obtained in this study.

Both materials showed low cohesion when tested in the direct shear apparatus compared to the values reported in the literature. MSWI slags have a higher friction angle value for ultimate and peak strength. MBT rejection friction angle is in the average of those in the revised literature.

5.4. Triaxial tests

Specimens with effective cell pressures of 50, 150, and 300 kPa were tested for each material in consolidated drained conditions using

the triaxial apparatus. Results for both materials are presented in separate sub-sections.

5.4.1. MBT rejection

Fig. 5a shows the deviator stress against the axial deformation of the specimens during the tests. In contrast to direct shear testing, failure was not attained in triaxial tests. This behavior is similar to the reported behavior of raw MSW found in the literature review but with a less noticeable effect of the fiber reinforcement, with curves almost linear and with no upward concavity. Due to that, mobilized shear strength values for different strain levels were obtained. In this case, the linear Mohr-Coulomb model was used to analyze the tests, as the observed difference between models in shear testing was not relevant, and the behavior of the material was almost linear. Figure A.8 (Supplementary Material) shows the stress paths in the q, p' Lambe's plane, with $q = \frac{\sigma'_1 - \sigma'_3}{2}$ and $p' = \frac{\sigma'_1 + \sigma'_3}{2}$, along with the linear envelopes obtained for strain values of 5, 10, 15, 20, and 25%. Mohr-Coulomb numerical parameter values are listed in Table A.11 (Supplementary Material). Additionally, secant Young's moduli were obtained for the latter strain levels and indicated in Table A.12 (Supplementary Material).

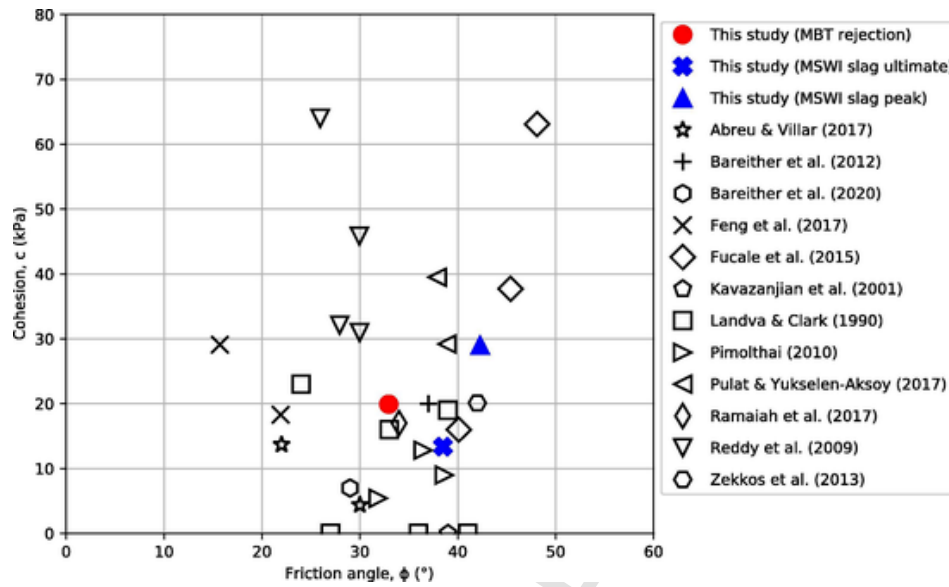


Fig. 4. Shear strength parameters obtained using direct shear tests.

Fig. 5b presents the volume change registered for each specimen against the axial strain. Poisson’s ratio can also be obtained by adjusting a line to the initial part of volume change plots, considering that it is an elastic zone. In this case, the parameter value does not depend on the effective cell pressure, and thus, the average value of the values obtained for each specimen was considered the value as the Poisson’s ratio for the material. Assuming small strains, the value of the Poisson ratio for each material was obtained using equation (3).

$$\epsilon_v = -(1 - 2\nu) \cdot \epsilon_a \quad (3)$$

Yielding in triaxial tests occur in one of the edges of the yielding surface defined by the generalized Mohr-Coulomb criterion in 3D, with $\sigma'_2 = \sigma'_3$. This produces the indetermination of the normal vector. Cimentada (2009) proposed the usage of the middle vector to obtain dilatancy angle (ψ), and hence this parameter can be obtained by adjusting the final points of each curve to equation (4).

$$\Delta \epsilon_v^p = \frac{2 \cdot \sin(\psi)}{1 - \sin(\psi)} \cdot \Delta \epsilon_a^p \quad (4)$$

with: ϵ_v^p = plastic volumetric strain, and ϵ_a^p = plastic axial strain.

Dilatancy angles (ψ) obtained using equation (4) and Poisson’s ratio (ν) obtained using equation (3) for each tested specimen are listed in Table A.12 in the Supplementary Material.

5.4.2. MSWI slags

Saturating specimens prepared with samples of MSWI slags using the procedure described above was challenging. Skempton’s pore pressure parameter (B) values in the range of 0.55 and 0.85 were initially obtained. It was also observed that these values decreased with time, and thus saturation degree changed in the same manner. To properly saturate specimens, samples were kept submerged in water for a month before the specimen preparation procedure started. After this, values of B in the range of 0.83 and 0.99 were attained. The great internal porosity of the particles could explain this improvement in saturation. Particle pores are initially filled with air and water can not access these pores during specimen preparation. However, in the consolidation process, with the backpressure provided, water finally gets into the pores, releasing air and causing saturation degree to decrease. Both kinds of samples were tested, showing similar behavior despite the change in the saturation degree. Only the results obtained with an appropriate value of the Skempton’s pore pressure parameter are de-

scribed below; further information on the process and the obtained results of the rest of the tests are described in Lapeña-Mañero (2017).

Fig. 5c shows the deviator stress against axial strain. Contrary to what was observed in direct shear tests, specimens did not show peak strength. The ultimate stress value was reached for strains between 13% and 22%, with increasing values for increasing effective cell pressure. Only the specimen tested with an effective cell pressure of 300 kPa shows a slight reduction in deviator stress after the maximum. However, this reduction was obtained for an axial strain over 25%, and it is more likely attributable to the effect on the test of large deformations than to a post-peak softening behavior of the material. The linear Mohr-Coulomb strength envelope for failure and axial strain values of 5%, 10%, and 15% are shown in Figure A.9 (Supplementary Materials), and the values of the Mohr-Coulomb parameters are summarized in Table A.11 (Supplementary Material). Additionally, secant Young’s moduli were obtained for the strain levels listed above.

In Fig. 5d, volume change against axial strain curves are plotted. The figure indicates that the specimen with the lower cell pressure ($p'_0 = 50$ kPa) volume increased during failure while specimen for $p'_0 = 300$ kPa reduced its volume on failure. The volume in the specimen with the intermediate effective cell pressure ($p'_0 = 150$ kPa), remained approximately constant. The values obtained for the secant Young’s moduli, Poisson’s ratios, and dilatancy angles are presented in the Supplementary Material (Table A.12).

5.4.3. Comparison with reported results

MBT rejection is, both in behavior and appearance, more similar to un-treated MSW than MSWI slags. Despite having less amount of fibers and these being shorter than in raw MSW, the material showed strain hardening. However, the gavel-like material produced in the MSWI plant behaved like a granular soil.

Fig. 6 shows a $c - \phi$ chart with the values of the mobilized parameters obtained for both materials at different strain levels. MBT rejection is plotted as circles, while MSWI is plotted with squares, with different colors for both materials representing the axial strain level.

The MBT rejection sample’s friction angle and cohesion Mohr-Coulomb parameter values raise with axial strain. The cohesion obtained for an axial strain of 25% approximately triples the value for 5% strain. Regarding the friction angle, the tendency is the same, with an increasing value of the mobilized friction angle with strain; it raises from 20° to 28.7°, a 143% increase.

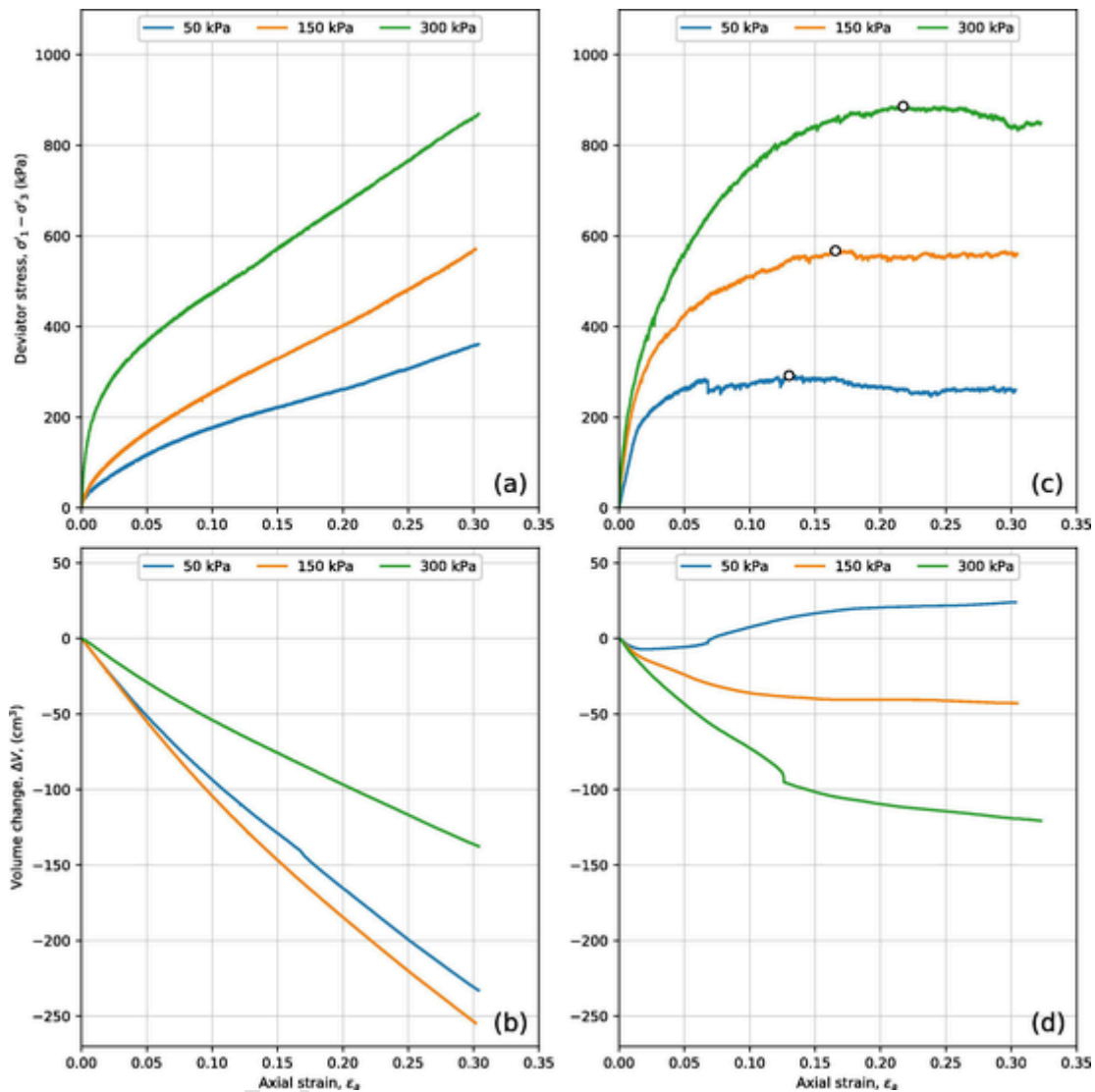


Fig. 5. Triaxial tests results, a) deviator stress against axial strain for the MBT rejection, b) volume change against axial strain in triaxial tests for MBT rejection, c) deviator stress against axial strain for MSWI slags in triaxial testing, and d) volume change against axial strain for MSWI slags in triaxial testing.

On the other hand, the behavior of MSWI slags is different. While they show the same tendency of increasing friction angle with strain, cohesion decreases for increasing strain values. The friction angle value varies from 21.8° for a value of axial strain of 5% to 32.8° when failure is reached. Cohesion values range from 0 to 70 kPa for 5% strain and failure, respectively.

As wastes do not usually reach failure during triaxial tests, mobilized shear strength parameter values were reported in some of the studies used for the comparison. In these cases, the mobilized shear strength for 20% axial strain was used as strength parameters for comparison. Fig. 7 summarizes the reported values of the Mohr-Coulomb parameters obtained using triaxial tests found in the literature and the values obtained in this investigation. Due to the variability in composition and applied treatment, value ranges for both parameters are wide, with cohesion ranging from 0 to 70 kPa and friction angle from 14° to 54.5°. The MBT rejection tested has a high cohesion value and an average friction angle, while the MSWI slags show approximately the same cohesion as MBT rejection and a higher value of the friction angle. The results obtained for the tested materials indicate that the shear strength of both materials can be considered high compared to the reported values found in the literature.

Fig. 8 shows the mobilized shear strength parameters at different axial strain levels obtained using triaxial tests in this study, along with those found in the literature. In the figure, markers indicate the reference where data were extracted and color the axial strain level.

All the materials found in the literature with mobilized parameter values for shear strength parameters correspond to non-treated MSW or MBT-treated wastes. In these cases, the same tendency of increasing both friction angle of cohesion with strain was found. In Fig. 8, strips of points representing the same axial strain levels can be identified. As stated above, the behavior of MSWI slag differs, with increasing friction angle and decreasing cohesion with axial strain.

6. Conclusions

The application of pre-treatments to waste before landfilling is common in current waste management operations and these treatments varies the physicochemical properties of wastes significantly, changing their behavior compared to traditional MSW. In addition, the information available in the literature about the mechanical properties of treated residues is scarce, as most research focused on raw MSW, making it necessary to establish appropriate shear strength envelopes for materials subjected to different pre-treatments.

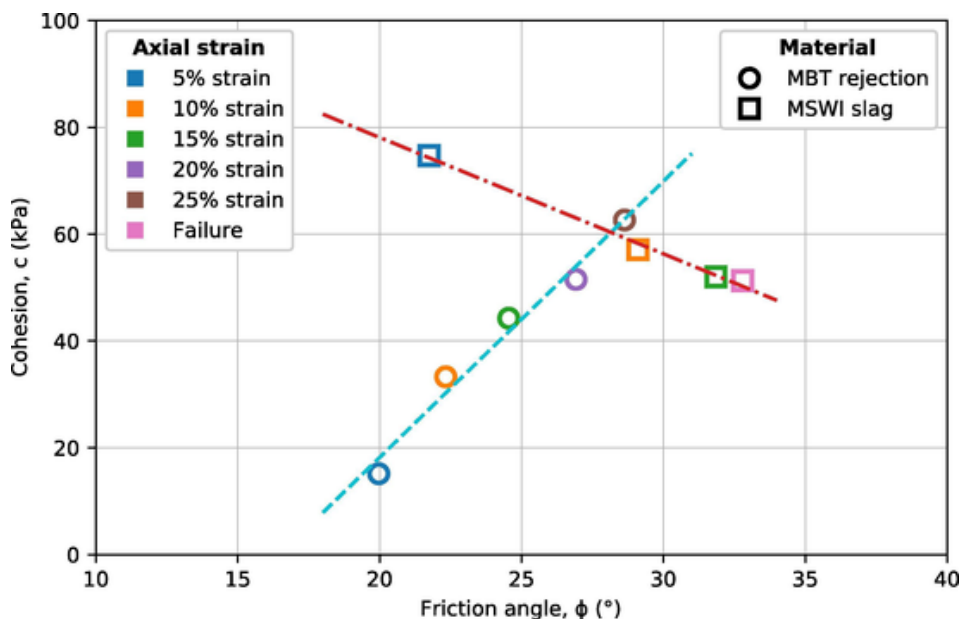


Fig. 6. Mohr-Coulomb parameter values against strain for both materials.

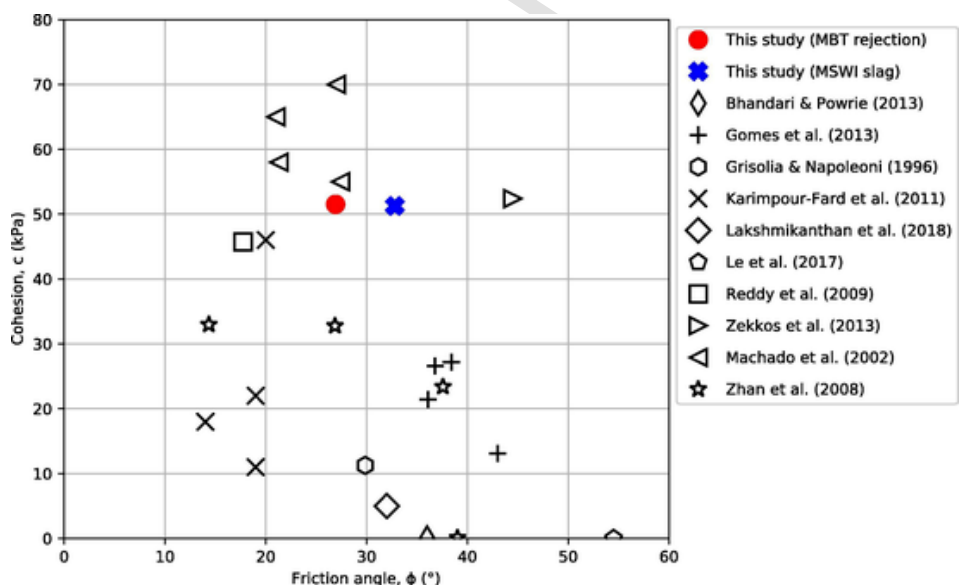


Fig. 7. Shear strength parameters at failure obtained using triaxial tests.

In this work, direct shear tests and consolidated drained triaxial tests have been performed on fresh samples of two pre-treated wastes obtained directly from the stockpiles where wastes are stored before being landfilled at the integral treatment plant from the Meruelo Environmental Complex in Cantabria, northern Spain. The materials tested corresponded with the rejection from the MBT and the slags produced in the incineration facility (MSWI). A method to prepare cylindrical specimens for triaxial testing based on freezing the samples has been developed and used successfully for the testing campaign on both materials.

Unlike in raw MSW, it was possible to reach failure during the test for both materials in direct shear testing. In triaxial testing of MBT rejection, failure was not reached, but strain hardening was less noticeable than in raw MSW. This behavior can be explained by the decrease in the amount of fibers produced by the treatments.

MBT rejection is similar in terms of appearance and behavior to traditional MSW, with smaller particle size due to the shredding and screening processes applied to the material in the treatment. The treatment also significantly reduces the amount of fibrous materials in the

waste mass, hence the reinforcement effect fibers have in the behavior of non-treated MSW. In direct shear testing, the obtained strength can be characterized by a cohesion of $c = 20$ kPa and a friction angle $\phi = 33^\circ$, while for triaxial testing, the mobilized parameters for 25% strain are $c_{25} = 62.6$ kPa and $\phi_{25} = 28.6^\circ$.

MSWI slags are similar to gravelly soil with a sandy fraction with fragile particles. The material showed both peak and ultimate strength on direct shear test, with strength parameters values of $c_{peak} = 29$ kPa and $\phi_{peak} = 42.3^\circ$ for peak strength and $c_{ult} = 13.4$ kPa and $\phi_{ult} = 38.5^\circ$ for ultimate strength. In triaxial testing, the material showed no peak strength, and the strength envelope is characterized by a cohesion of $c = 50.7$ kPa and a friction angle of $\phi = 34.6^\circ$.

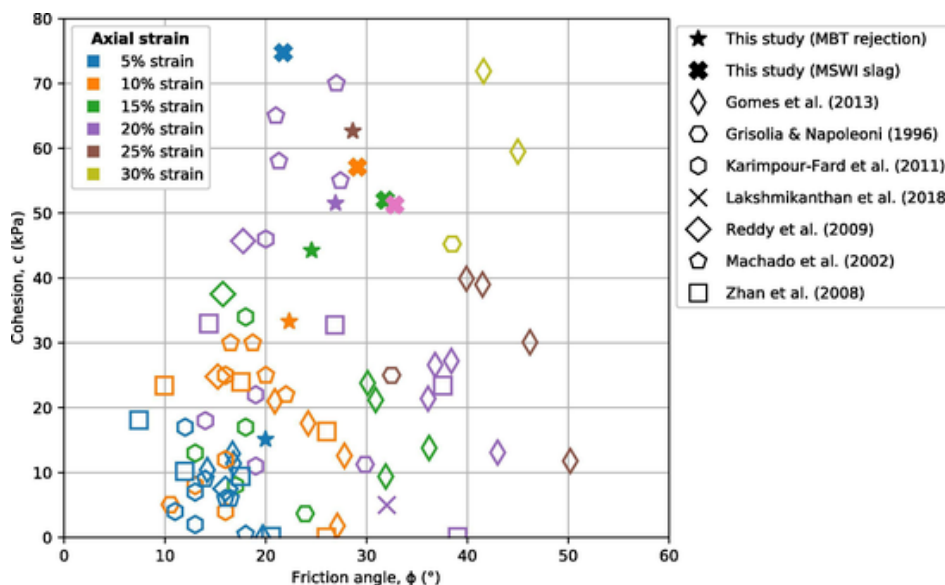


Fig. 8. Mobilized shear strength for different axial strain values.

Declaration of Competing Interest

The authors declare that they have no known competing financial interests or personal relationships that could have appeared to influence the work reported in this paper.

Acknowledgments

This work was supported by the Spanish Ministry of Economy and Competitiveness [grant number BIA2012-34956]; the Spanish Ministry of Education, Culture and Sports [grant number FPU12/05530]; and the Dirección de Investigación de la Universidad Católica de la Santísima Concepción [grant number INIDIN 07/2019]. The authors would also like to thank Tircantabria S.L.U. for their support during the investigation, especially on sampling.

Appendix A. Supplementary material

Supplementary data to this article can be found online at <https://doi.org/10.1016/j.wasman.2022.08.026>.

References

- Abreu, A.E.S., Vilar, O.M., 2017. Influence of composition and degradation on the shear strength of municipal solid waste. *Waste Manage.* 68, 263–274. <https://doi.org/10.1016/j.wasman.2017.05.038>.
- Athanasopoulos, G.A., 2008. Laboratory Testing of Municipal Solid Waste. *Geotechnical Characterization, Field Measurement, and Laboratory Testing of Municipal Solid Waste*. 195–205. [https://doi.org/10.1061/41146\(395\)7](https://doi.org/10.1061/41146(395)7).
- Bareither, C.A., Benson, C.H., Edil, T.B., 2008. Comparison of shear strength of sand backfills measured in small-scale and large-scale direct shear tests. *Can. Geotech. J.* 45, 1224–1236. <https://doi.org/10.1139/T08-058>.
- Bareither, C.A., Benson, C.H., Edil, T.B., 2012. Effects of waste composition and decomposition on the shear strength of municipal solid waste. *J. Geotech. Geoenviron. Eng.* 138, 1161–1174. [https://doi.org/10.1061/\(ASCE\)GT.1943-5606.0000702](https://doi.org/10.1061/(ASCE)GT.1943-5606.0000702).
- Bareither, C.A., Benson, C.H., Rohlfs, E.M., Scalia, J., 2020. Hydraulic and mechanical behavior of municipal solid waste and high-moisture waste mixtures. *Waste Manage.* 105, 540–549. <https://doi.org/10.1016/j.wasman.2020.02.030>.
- Barton, N., 1976. The shear strength of rock and rock joints. *Int. J. Rock Mech. Mining Sci. Geomechanics Abstracts* 13, 255–279. [https://doi.org/10.1016/0148-9062\(76\)90003-6](https://doi.org/10.1016/0148-9062(76)90003-6).
- Bhandari, A.R., Powrie, W., 2013. Behavior of an MBT waste in monotonic triaxial shear tests. *Waste Manage.* 33, 881–891. <https://doi.org/10.1016/j.wasman.2012.11.009>.
- Bray, J.D., Zekkos, D., Kavazanjian, E., Athanasopoulos, G.A., Riemer, M.F., 2009. Shear strength of municipal solid waste. *J. Geotech. Geoenviron. Eng.* 135 (6), 709–722.
- Caicedo, B., Giraldo, E., Yamin, L., Soler, N., 2002. The landslide of Dona Juana Landfill in Bogota. A case study. Presented at the Fourth international congress on environmental geotechnics (4th ICEG), Río de Janeiro (Brazil).
- Chugh, A.K., Stark, T.D., DeJong, K.A., 2007. Reanalysis of a municipal landfill slope failure near Cincinnati, Ohio. USA. *Can. Geotech. J.* 44, 33–53. <https://doi.org/10.1139/t06-089>.
- Cimentada Hernández, A.L., 2009. *Análisis experimental en modelo reducido de la consolidación radial y deformación de un suelo blando mejorado con columnas de gava*. University of Cantabria, Santander, Spain. Ph.D. Thesis.
- Di Lonardo, M.C., Lombardi, F., Gavasci, R., 2012. Characterization of MBT plants input and outputs: a review. *Rev. Environ. Sci. Bio/Technol.* 11, 353–363. <https://doi.org/10.1007/s11157-012-9299-2>.
- Dixon, N., Jones, D.R.V., 2005. Engineering properties of municipal solid waste. *Geotext. Geomembr.* 23, 205–233. <https://doi.org/10.1016/j.geotextmem.2004.11.002>.
- Dixon, N., Whittle, R.W., Jones, D.R.V., Ng'ambi, S., 2006. Pressuremeter tests in municipal solid waste: measurement of shear stiffness. *Géotechnique* 56, 211–222. <https://doi.org/10.1680/geot.2006.56.3.211>.
- Dorador, L., Villalobos, F.A., 2020. *Scalping techniques in geomechanical characterization of coarse granular materials*. *Obras y Proyectos* (28), 24–34.
- Eid, H.T., Stark, T.D., Douglas, E.W., Sherry, P.E., 2000. Municipal Solid Waste Slope Failure. I: waste and foundation soil properties. *J. Geotech. Geoenviron. Eng.* 126, 397–407. [https://doi.org/10.1061/\(ASCE\)1090-0241\(2000\)126:5\(397\)](https://doi.org/10.1061/(ASCE)1090-0241(2000)126:5(397)).
- Espinace, R., Farfán, J., 2016. *Desafíos en la estabilidad de nuevos rellenos sanitarios*. Presented at the IX Congreso Chileno de Ingeniería Geotécnica, Valdivia, Chile.
- European Council, 2018. Council Directive 1999/31/EC of 26 April 1999 on the landfill of waste. European Council.
- Feng, S.-J., Gao, K.-W., Chen, Y.-X., Li, Y., Zhang, L.M., Chen, H.X., 2017. Geotechnical properties of municipal solid waste at Laogang Landfill, China. *Waste Manage.* 63, 354–365. <https://doi.org/10.1016/j.wasman.2016.09.016>.
- Fricke, K., Santen, H., Wallmann, R., 2005. Comparison of selected aerobic and anaerobic procedures for MSW treatment. *Waste Manage.* 25, 799–810. <https://doi.org/10.1016/j.wasman.2004.12.018>.
- Fucale, S., Jucá, J.F.T., Muennich, K., 2015. *The Mechanical Behavior of MBT- Waste*. *Electron. J. Geotech. Eng.* 20, 5927–5937.
- Gomes, C., Lopes, M.L., Oliveira, P.J.V., 2013. Municipal solid waste shear strength parameters defined through laboratorial and in situ tests. *J. Air Waste Manag. Assoc.* 63, 1352–1368. <https://doi.org/10.1080/10962247.2013.813876>.
- Grisolia, M., Napoleoni, Q., 1996. Geotechnical characterization of municipal solid waste: Choice of design parameters., in: *Proceedings of the Second International Congress on Environmental Geotechnics*. Bankelma, Osaka, Japan, pp. 641–646.
- Huvaj-Sarihan, N., Stark, T.D., 2008. Back-Analyses of Landfill Slope Failures. Presented at the Sixth International Conference on Case Histories in Geotechnical Engineering, Arlington, Virginia, U.S.A.
- Jiang, J.-C., Baker, R., Yamagami, T., 2003. The effect of strength envelope nonlinearity on slope stability computations. *Can. Geotech. J.* 40, 308–325. <https://doi.org/10.1139/t02-111>.
- Karimpour-Fard, M., Machado, S.L., Shariatmadari, N., Noorzad, A., 2011. A laboratory study on the MSW mechanical behavior in triaxial apparatus. *Waste Manage.* 31, 1807–1819. <https://doi.org/10.1016/j.wasman.2011.03.011>.
- Kavazanjian, E., Hendron, D., Corcoran, G.T., 2001. Strength and Stability of Bioreactor Landfills, in: *Proceedings of the 6th Annual Landfill Symposium, Solid Waste Association of North America*. Silver Springs, Maryland, U.S.A., pp. 63–72.
- Kavazanjian, E., Matasovic, N., Bonaparte, R., Schmertmann, G.R., 1995. *Evaluation of MSW properties for seismic analysis*. *Geotechnical Special Publication*. ASCE 1126–1141.
- Kölsch, F., 1995. Material values for some mechanical properties of domestic waste, in: *Proceedings of the Fifth International Landfill Symposium*. CISA ed., Cagliari, Italy,

- pp. 711–726.
- Lakshmikanthan, P., Sughosh, P., Sivakumar Babu, G.L., 2018. Studies on characterization of mechanically biologically treated waste from bangalore city. *Indian Geotechnical J.* 48, 293–304. <https://doi.org/10.1007/s40098-018-0296-4>.
- Landva, A.O., Clark, J., 1990. Geotechnics of Waste Fill, in: Landva, A., Knowles, G. (Eds.), *Geotechnics of Waste Fills—Theory and Practice*. ASTM International, West Conshohocken, PA, pp. 86–103. <https://doi.org/10.1520/STP25301S>.
- Lapeña-Mañero, P., 2017. Caracterización experimental del comportamiento resistente de vertederos de residuos sólidos urbanos convencionales (R.S.U.) y sometidos a pre-tratamiento (R.S.U.-M.B.T.). University of Cantabria, Santander, Spain. Ph.D. Thesis.
- Lavigne, F., Wassmer, P., Gomez, C., Davies, T.A., Sri Hadmoko, D., Iskandarsyah, T.Y.W.M., Gaillard, J., Fort, M., Texier, P., Boun Heng, M., Pratomo, I., 2014. The 21 February 2005, catastrophic waste avalanche at Leuwigajah dumpsite, Bandung, Indonesia. *Geoenvironmental Disasters* 1, 10. <https://doi.org/10.1186/s40677-014-0010-5>.
- Le, N.H., Abriak, N.E., Binetruy, C., Benzerzour, M., Nguyen, S.-T., 2017. Mechanical behavior of municipal solid waste incinerator bottom ash: Results from triaxial tests. *Waste Manage.* 65, 37–46. <https://doi.org/10.1016/j.wasman.2017.03.045>.
- López, A., García, M., Esteban-García, A.L., Cuartas, M., Molleda, A., Lobo, A., 2018. Emissions from mechanically biologically treated waste landfills at field scale. *Int. J. Environ. Sci. Technol.* 15, 1285–1300. <https://doi.org/10.1007/s13762-017-1497-6>.
- Machado, S.L., Carvalho, M.F., Vilar, O.M., 2002. Constitutive model for municipal solid waste. *J. Geotech. Geoenviron. Eng.* 128, 940–951. [https://doi.org/10.1061/\(ASCE\)1090-0241\(2002\)128:11\(940\)](https://doi.org/10.1061/(ASCE)1090-0241(2002)128:11(940)).
- Maksimovic, M., 1989. Non-linear failure envelope for soils. *J. Geotechnical Eng.* 115, 581–586. [https://doi.org/10.1061/\(ASCE\)0733-9410\(1989\)115:4\(581\)](https://doi.org/10.1061/(ASCE)0733-9410(1989)115:4(581)).
- Manassero, M., Van Impe, W.F., Bouazza, A., 1996. Waste disposal and containment, in: *Proceedings of the Second International Congress on Environmental Geotechnics*. Osaka (Japan), pp. 1425–1474.
- Martínez-Bacas, B.M., Konietzky, H., Cañizal, J., Sagaseta, C., 2011. A new constitutive model for textured geomembrane/geotextile interfaces. *Geotext. Geomembr.* 29, 137–148. <https://doi.org/10.1016/j.geotexmem.2010.10.014>.
- Merry, S.M., Kavazanjian, E., Fritz, W.U., 2005. Reconnaissance of the July 10, 2000, Payatas Landfill Failure. *J. Perform. Constr. Facil* 19 (2), 100–107.
- Mitchell, J.K., Chang, M., Seed, R.B., 1993. The Kettleman Hills Landfill Failure: A Retrospective View of the Failure Investigations and Lessons Learned. Presented at the Third International Conference on Case Histories in Geotechnical Engineering, St. Louis, Missouri (U.S.A.).
- Molleda, A., 2017. Detailed characteristics and landfill pollution potential of rejects from mechanical-biological treatment of municipal waste: the spanish case. University of Cantabria, Santander, Spain. Ph.D. Thesis.
- Molleda, A., López, A., Cuartas, M., Lobo, A., 2020. Release of pollutants in MBT landfills: laboratory versus field. *Chemosphere* 249, 126145. <https://doi.org/10.1016/j.chemosphere.2020.126145>.
- Palma, J., 1995. Comportamiento geotécnico de vertederos controlados de residuos sólidos urbanos. University of Cantabria, Santander, Spain. Ph.D. Thesis.
- Peng, R., Hou, Y., Zhan, L., Yao, Y., 2016. Back-analyses of landfill instability induced by high water level: case study of shenzhen landfill. *Int. J. Environ. Res. Public Health* 13 (1), 126.
- Perry, J., 1994. A technique for defining non-linear shear strength envelopes, and their incorporation in a slope stability method of analysis. *Q. J. Eng. Geol. Hydrogeol.* 27, 231–241. <https://doi.org/10.1144/GSL.QJEGH.1994.027.P3.04>.
- Pimolthai, P., 2010. Comparative study of physical and chemical characteristics of the mechanically and biologically treated waste from Luxembourg, Germany and Thailand. Trier University, Trier, Germany. Ph.D. Thesis.
- Pulat, H.F., Yukselen-Aksoy, Y., 2017. Factors affecting the shear strength behavior of municipal solid wastes. *Waste Manage.* 69, 215–224. <https://doi.org/10.1016/j.wasman.2017.08.030>.
- Ramaiah, B.J., Ramana, G.V., Datta, M., 2017. Mechanical characterization of municipal solid waste from two waste dumps at Delhi, India. *Waste Manage.* 68, 275–291. <https://doi.org/10.1016/j.wasman.2017.05.055>.
- Reddy, K.R., Hettiarachchi, H., Parakalla, N.S., Gangathulasi, J., Bogner, J.E., 2009. Geotechnical properties of fresh municipal solid waste at Orchard Hills Landfill, USA. *Waste Manage.* 29, 952–959. <https://doi.org/10.1016/j.wasman.2008.05.011>.
- Robinson, H.D., Knox, K., Bone, B.D., Picken, A., 2005. Leachate quality from landfilled MBT waste. *Waste Manage.* 25, 383–391. <https://doi.org/10.1016/j.wasman.2005.02.003>.
- Rotter, V.S., Kost, T., Winkler, J., Bilitewski, B., 2004. Material flow analysis of RDF-production processes. *Waste Manage.* 24, 1005–1021. <https://doi.org/10.1016/j.wasman.2004.07.015>.
- Sánchez-Alciturri, J.M., Palma, J., Sagaseta, C., Cañizal, J., 1993. Mechanical properties of wastes in a sanitary landfill, in: *Waste Disposal by Landfill*. R.W. Sarsby, ed., Bolton, U.K., pp. 357–364.
- Siddiqui, A.A., Powrie, W., Richards, D.J., 2013. Settlement characteristics of mechanically biologically treated wastes. *J. Geotech. Geoenviron. Eng.* 139, 1676–1689. [https://doi.org/10.1061/\(ASCE\)GT.1943-5606.0000918](https://doi.org/10.1061/(ASCE)GT.1943-5606.0000918).
- Sivakumar Babu, G.L., Lakshmikanthan, P., Santhosh, L.G., 2015. Shear strength characteristics of mechanically biologically treated municipal solid waste (MBT-MSW) from Bangalore. *Waste Manage.* 39, 63–70. <https://doi.org/10.1016/j.wasman.2015.02.013>.
- Stark, T.D., Eid, H.T., Evans, W.D., Sherry, P.E., 2000. Municipal solid waste slope failure. II: stability analyses. *J. Geotech. Geoenviron. Eng.* 126, 408–419. [https://doi.org/10.1061/\(ASCE\)1090-0241\(2000\)126:5\(408\)](https://doi.org/10.1061/(ASCE)1090-0241(2000)126:5(408)).
- Stark, T.D., Huvaj-Sarihan, N., Li, G., 2009. Shear strength of municipal solid waste for stability analyses. *Environ. Geol.* 57, 1911–1923. <https://doi.org/10.1007/s00254-008-1480-0>.
- Velis, C.A., Longhurst, P.J., Drew, G.H., Smith, R., Pollard, S.J.T., 2010. Production and quality assurance of solid recovered fuels using mechanical—biological treatment (MBT) of waste: a comprehensive assessment. *Critical Rev. Environ. Sci. Technol.* 40, 979–1105. <https://doi.org/10.1080/10643380802586980>.
- Yang, Y., Gao, F., Lai, Y., 2013. Modified Hoek-Brown criterion for non-linear strength of frozen soil. *Cold Reg. Sci. Technol.* 86, 98–103. <https://doi.org/10.1016/j.coldregions.2012.10.010>.
- Zekkos, D., Athanopoulos, G.A., Bray, J.D., Grizi, A., Theodoratos, A., 2010. Large-scale direct shear testing of municipal solid waste. *Waste Manage.* 30, 1544–1555. <https://doi.org/10.1016/j.wasman.2010.01.024>.
- Zekkos, D., Bray, J.D., Athanopoulos, G.A., Riemer, M.F., Kavazanjian, E., Founta, P.A., Grizi, A., 2007a. Compositional and loading rate effects on the shear strength of municipal solid waste, in: *Proceedings of the Fourth International Conference on Earthquake Geotechnical Engineering*. Thessaloniki (Greece).
- Zekkos, D., Bray, J.D., Kavazanjian, E., Matasovic, N., Rathje, E.M., Riemer, M.F., Stokoe, K.H., 2006. Unit Weight of Municipal Solid Waste. *J. Geotech. Geoenviron. Eng.* 132 (10), 1250–1261.
- Zekkos, D., Bray, J.D., Riemer, M.F., Kavazanjian, E., Athanopoulos, G.A., 2007b. Response of municipal solid-waste from Tri-Cities landfill in triaxial compression, in: *Proceedings of Th Eleventh International Waste Management and Landfill Symposium*. Cagliari, Italy.
- Zekkos, D., Kabalan, M., Syal, S.M., Hambright, M., Sahadewa, A., 2013. Geotechnical characterization of a Municipal Solid Waste Incineration Ash from a Michigan monofill. *Waste Manage.* 33, 1442–1450. <https://doi.org/10.1016/j.wasman.2013.02.009>.
- Zhan, T.L.T., Chen, Y.M., Ling, W.A., 2008. Shear strength characterization of municipal solid waste at the Suzhou landfill, China. *Eng. Geol.* 97, 97–111. <https://doi.org/10.1016/j.enggeo.2007.11.006>.
- Zhao, Y.R., Xie, Q., Wang, G.L., Zhang, Y.J., Zhang, Y.X., Su, W., 2014. A study of shear strength properties of municipal solid waste in Chongqing landfill. *China Environ. Sci. Pollution Res.* 21, 12605–12615. <https://doi.org/10.1007/s11356-014-3183-2>.